Suppression of Electro-Osmotic Flow by Surface Roughness

R. J. Messinger and T. M. Squires*

Department of Chemical Engineering, University of California, Santa Barbara, California 93106, USA

(Received 12 June 2010; revised manuscript received 12 August 2010; published 30 September 2010)

We show that nanoscale surface roughness, which commonly occurs on microfabricated metal electrodes, can significantly suppress electro-osmotic flows when excess surface conductivity is appreciable. We demonstrate the physical mechanism for electro-osmotic flow suppression due to surface curvature, compute the effects of varying surface conductivity and roughness amplitudes on the slip velocities of a model system, and identify scalings for flow suppression in different regimes of surface conduction. We suggest that roughness may be one factor that contributes to large discrepancies observed between classical electrokinetic theory and modern microfluidic experiments.

DOI: 10.1103/PhysRevLett.105.144503 PACS numbers: 47.61.−k, 47.57.jd, 85.85.+j

Electrokinetic flows are established when an electric field forces the diffuse ionic cloud adjacent to a charged surface in a liquid electrolyte into motion. Micro- and nanofluidics have driven a resurgence in electrokinetic research, with applications as diverse as directed assembly of colloids, energy conversion and storage, biological and chemical sensors, pumps, and electrophoretic separations for genomics and proteomics [1].

In electro-osmotic flow, fluid appears to "slip" parallel to charged surfaces with a velocity given by the classical Helmholtz-Smoluchowski formula,

$$u_{\mathrm{HS}} = -\frac{\epsilon\zeta}{\mu}E_{\|}, \tag{1}$$

where ϵ and μ are the permittivity and viscosity of the liquid, ζ is the potential drop across the diffuse screening cloud, and $E_{\|}$ is the tangential component of the electric field [2]. Although electrokinetics marks its origins over two centuries ago, significant discrepancies still exist between theory and experiments [3], particularly with nonlinear "induced charge" effects, where the induced ζ can be predicted, and thus compared directly against experiments [4]. Various mechanisms have been proposed to account for deviations from (1), such as ion steric effects [3], ion-ion couplings [5], electroviscous effects [6], surface contamination [7], and Faradaic reactions [8].

Surface geometry might also be expected to play a role in electrokinetic transport. Morrison [9], however, showed the electrophoretic velocity of colloidal particles to be independent of shape and size, provided that ζ is constant and screening length λ_D is thin relative to the colloid radius. An analogous argument shows electro-osmotic "similitude": electro-osmotic flow through insulating microchannels with constant ζ and thin double layers is everywhere proportional to the local electric field vector, regardless of channel geometry [10]. Investigations of micron-scale roughness of amplitude a_r for nonconstant ζ and thin double layers ($\lambda_D \ll a_r$) [11], constant ζ and finite but thin double layers [12], and randomly generated roughness with constant ζ and $\lambda_D \sim a_r$ [13] indicate that roughness may reduce electro-osmotic flow. Molecular dynamic simulations of nanometer and subnanometer roughness for $\lambda_D \sim a_r$ also suggest that roughness may decrease electro-osmotic slip [14]. However, a general, physical understanding for electrokinetic flow suppression due to roughness is lacking, especially under common experimental conditions for microfabricated systems, where surface conduction may play a crucial role.

Here we show that even nanoscale surface roughness can suppress electrokinetic flows whenever excess surface conductivity within the double-layer is appreciable, even for thin double layers ($\lambda_D \ll a_r$) and constant ζ. The influence of surface conduction on electrophoresis was first noted by Bikerman [15], Dukhin and Deryaguin [16], and is parametrized by the Dukhin number [17],

$$\mathrm{Du} = \sigma_s/(\sigma_B a), \tag{2}$$

where σ_s and σ_B are the surface and bulk conductivities and a is the colloid radius. Indeed, the electrophoretic mobility of a spherical colloid shows a maximum at $\mathrm{Du} \sim \mathcal{O}(1)$ [18]. For rough surfaces, the roughness curvature itself provides the relevant length scale for Du. Evaporated metal electrodes of, e.g., $a_e \sim \mathcal{O}(10)$ μm dimension routinely show $a_r \sim \mathcal{O}(10)$ nm rough features [19], whose "invisible" curvature would make Du greater than naively expected from electrode geometry by a factor of $a_e/a_r \sim 10^3$. Nanoscale roughness, then, can cause surface conduction to play an unexpectedly strong role.

The mechanism of electro-osmotic flow suppression by surface roughness is shown in Fig. 1. A field $\mathbf{E}^{\infty}$ applied tangent to a charged, flat surface forces the ions within the charged double layer into motion, resulting in a slip velocity $\mathbf{u}_{\mathrm{HS}}^{\infty} = -\epsilon\zeta\mathbf{E}^{\infty}/\mu$ [Fig. 1(a)]. However, when $\mathbf{E}^{\infty}$ is applied over a sinusoidally rough surface (amplitude a_r and period L), the tangential component $E_{\|}$ at the surface is inhomogeneous, being strongest at roughness maxima and weakest at minima [Fig. 1(b)], yielding an inhomogeneous slip velocity $u_{\|}$. Remarkably, under conditions of weak

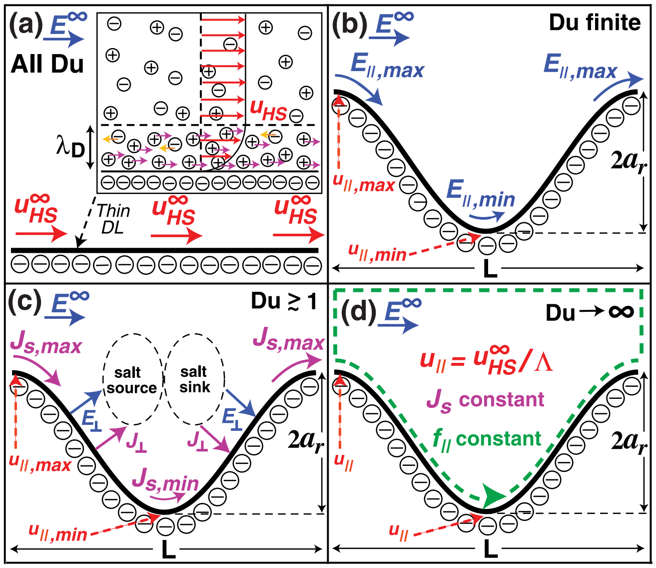

FIG. 1 (color online). (a) An applied electric field $\mathbf{E}^\infty$ forces the ion cloud around a flat charged plate into motion, driving an electro-osmotic "slip" velocity $\mathbf{u}^\infty_{\rm HS}$. (b) Curvature results in an inhomogeneous tangential $E_\parallel$ and slip velocity $u_\parallel$. (c) Appreciable surface conductivity ($\mathrm{Du} \gtrsim 1$) gives rise to gradients in the excess counterion surface current J_s, and conservation requires normal flux of counterions $\mathbf{J}_\perp$ and field lines $\mathbf{E}_\perp$. This normal flux reduces $E_\parallel$ and $u_\parallel$, yielding $\mathbf{U}^\infty_{\rm EO} < \mathbf{u}^\infty_{\rm HS}$. Additionally, $\mathbf{J}_\perp$ creates salt sources and sinks. (d) For strong surface conductivity ($\mathrm{Du} \to \infty$), ion transport in the double layer is rate-limited by exchange with the bulk, requiring a divergence-free surface current J_s and yielding a constant slip velocity $u_\parallel = u^\infty_{\rm HS}/\Lambda$.

excess surface conductivity ($\mathrm{Du} \ll 1$) and thin double layers ($\lambda_D/a_r \ll 1$), the far-field electro-osmotic slip velocity $\mathbf{U}^\infty_{\rm EO}$ is identical to that over a smooth surface ($\mathbf{U}^\infty_{\rm EO} = \mathbf{u}^\infty_{\rm HS}$). This result reflects similitude [9,10], and holds generally when $\mathbf{E}$ obeys a no-flux boundary condition at solid walls (i.e., $\mathrm{Du} \ll 1$).

As excess surface conduction becomes appreciable ($\mathrm{Du} \gtrsim 1$), however, the inhomogeneous tangential field $\mathbf{E}_\parallel$ drives an inhomogeneous surface current $\mathbf{J}_s \sim \sigma_s \mathbf{E}_\parallel$ [Fig. 1(c)]. For ions to be conserved, its divergence $\nabla_s \cdot \mathbf{J}_s \sim \sigma_s E^\infty/a_r$ must be balanced by bulk ion flux to or from the double layer, $\mathbf{J}_\perp = \sigma_B \mathbf{E}_\perp \sim \sigma_B E^\infty$. Appreciable surface conduction thus requires a normal counterion flux $\mathbf{J}_\perp$ and field $\mathbf{E}_\perp \sim (\sigma_s/\sigma_B a_r) E^\infty \sim \mathrm{Du} E^\infty$, which reduces both $E_\parallel$ and $u_\parallel$ to give $\mathbf{U}^\infty_{\rm EO} < \mathbf{u}^\infty_{\rm HS}$.

Normal ion flux to or from the bulk ($\mathbf{J}_\perp \sim \sigma_B E^\infty$) has an upper bound, however, and is simply too weak to accommodate any surface current divergence ($\nabla_s \cdot \mathbf{J}_s \sim \sigma_s E^\infty/a_r$) in the $\mathrm{Du} \gg 1$ limit of strong surface conduction. Instead, the bulk fields adjust to render the surface current $\mathbf{J}_s$ divergence-free. For J_s to be streamwise constant, so must the tangential force $f_\parallel \propto E_\parallel$ on double-layer ions. Since this force is irrotational [$\oint \mathbf{f} \cdot d\mathbf{l} = 0$, along the dashed line in Fig. 1(d)], $f_\parallel = f^\infty/\Lambda \propto E^\infty/\Lambda$, where Λ is the surface arclength per period L. This tangential force gives a constant "sliding wall" velocity,

$$u_\parallel = -\frac{1}{\Lambda}\frac{\epsilon\zeta E^\infty}{\mu} = \frac{u^\infty_{\rm HS}}{\Lambda}, \tag{3}$$

which is everywhere lower than $u^\infty_{\rm HS}$, and thus yields a far-field velocity $\mathbf{U}^\infty_{\rm EO} < \mathbf{u}^\infty_{\rm HS}$. The transition between the two asymptotic regimes for surface conduction (similitude for $\mathrm{Du} = 0$ and sliding wall for $\mathrm{Du} \to \infty$) occurs for $\mathrm{Du} \sim \mathcal{O}(1)$. Significantly, the length scale used to form Du in (2) is associated with the roughness itself (e.g., a_r or L), yielding a Du that can be orders of magnitude greater than expected from macroscopic geometry.

To treat electrokinetics over rough surfaces more generally, we work in the (common) limit of thin double layers ($\lambda_D/a_r \ll 1$), solving for the fields outside the double layer, and accounting for double-layer effects with effective boundary conditions. Since gradients in both electric potential ϕ and ion concentration $n_\pm$ drive ionic motion, we formulate a unified driving force using the electrochemical potentials $\mu_\pm$,

$$\mu_\pm = \pm e\phi + k_B T \ln(n_\pm), \tag{4}$$

where e is the fundamental charge, k_B is Boltzmann's constant, T is the temperature, and ± indicates positive and negative ions. The force on an ion, $\mathbf{f}_\pm = -\nabla\mu_\pm$, thus includes both electrostatic and entropic driving forces.

We compute in the weak field limit, $|\mathbf{E}^\infty| \ll |\zeta|/\lambda_D$, and linearize for weak perturbations to equilibrium quantities. Linearized chemical potentials [20] become

$$\delta\mu_\pm \approx \pm e\delta\phi + k_B T \frac{\delta n_\pm}{n^0}. \tag{5}$$

The perturbed electric potential $\delta\phi$ and bulk salt concentration δc may be recovered from $\delta\phi = (\delta\mu_+ - \delta\mu_-)/2e$ and $\delta c = (\delta\mu_+ + \delta\mu_-)n_0/2k_B T$, respectively.

Nondimensionalized governing equations [20] for the perturbed ion number density $\delta n_\pm$ and electric potential $\delta\phi$ (or equivalently $\delta\mu_\pm$), and fluid velocity $\mathbf{u}$, outside the (thin) double layers are simply given by

$$0 = \nabla^2 \delta\mu_\pm, \tag{6}$$

$$0 = -\nabla\delta p + \nabla^2 \mathbf{u}. \tag{7}$$

Effective boundary conditions for ion transport (6) are constructed by enforcing ion conservation within the double layer. As above [Fig. 1(c)], divergence in surface ion flux $\mathbf{J}_s$ drives a flux $\mathbf{J}_\perp$ into or out of the bulk, requiring

$$\hat{\mathbf{n}} \cdot \nabla\delta\mu_\pm = \mathrm{Du}_\pm \nabla_s^2 \delta\mu_\pm, \tag{8}$$

where $\mathrm{Du}_\pm = \sigma_s^\pm/(\sigma_B^\pm L)$ [20] represent distinct Dukhin numbers for counterions and coions.

Coions (here assumed negative) are essentially excluded from the double layer at appreciable surface conductivity, so $\mathrm{Du}_- \lesssim \lambda_D/L \approx 0$. Coions thus obey an effective

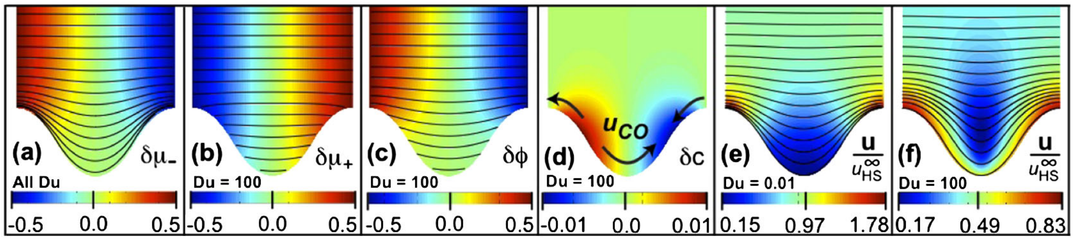

FIG. 2 (color online). Computations of $\delta\mu_\pm$, $\delta\phi$, δc, and $\mathbf{u}$ at selected values of excess surface conductivity (Du) for roughness length scales $a_r/L = 0.25$. (a) Coion field $\delta\mu_-$ for all Du, or equivalently, counterion field $\delta\mu_+$ for Du $\ll 1$. Counterion field $\delta\mu_+$ (b), electric potential $\delta\phi$ (c), and bulk salt concentration δc (d) for Du = 100. Velocity field $\mathbf{u}$ for Du = 0.01 (e) and Du = 100 (f), normalized by $u_{\rm HS}^{\infty}$. Solid black lines represent constant values of $\nabla\delta\mu_\pm$, $\nabla\delta\phi$, or velocity streamlines.

no-flux condition at the charged surface,

$$\hat{\mathbf{n}} \cdot \nabla\delta\mu_-|_\Gamma = 0. \tag{9}$$

Counterions, by contrast, obey a boundary condition

$$\hat{\mathbf{n}} \cdot \nabla\delta\mu_+|_\Gamma = \mathrm{Du}_\pm \nabla_s^2 \delta\mu_+|_\Gamma \tag{10}$$

that accounts for surface conduction: a nonuniform surface flux $\mathbf{J}_s^+$ requires an $\mathcal{O}(\mathrm{Du}_+)$ counterion flux into or out of the double layer.

Boundary conditions for the velocity field (7) relate slip velocities to ion forces $\mathbf{f}_\pm = -\nabla\delta\mu_\pm$, accounting for both electro-osmotic (from $\mathbf{E}$) and chemiosmotic (from salt concentration gradients) flows. For the Gouy-Chapman model of the double layer, O'Brien [18] derived $\mathbf{u}_\parallel = (\nabla_s\delta\phi)\zeta - 4(\nabla_s\delta c)\ln[\cosh(\zeta/4)]$, or

$$\mathbf{u}_\parallel|_\Gamma = -\frac{1}{2}(-\nabla_s\delta\mu_+ + \nabla_s\delta\mu_-)\zeta - 2(\nabla_s\delta\mu_+ + \nabla_s\delta\mu_-)\ln[\cosh(\zeta/4)]. \tag{11}$$

Du (coion and counterion contributions) may be computed using the Gouy-Chapman solution to the nonlinear Poisson-Boltzmann equation for the double layer [17],

$$\mathrm{Du} = \frac{4\lambda_D(1+m)}{L}\sinh^2(\zeta/4), \tag{12}$$

where $m = 2\epsilon(k_BT/e)^2/\eta D$ is the ratio between ion electroconvection to ion electromigration. In the computations below, we use $m = 0.34$ (for aqueous NaCl [18]), and arbitrarily choose $\lambda_D/L = 20$. Such choices do not affect our results qualitatively, but rather specify a Du-ζ relation. Since $\mathrm{Du}_+ \approx$ Du and $\mathrm{Du}_- \approx 0$ for Du $\gtrsim 1$, we use Du and Du_+ interchangeably.

Figure 2 shows $\delta\mu_\pm$, $\delta\phi$, δc, and $\mathbf{u}$, obtained by solving (6) and (7) subject to (8)–(11) using the finite-element package COMSOL, which verify the physical mechanisms in Fig. 1. The coion potential $\delta\mu_-$ for all Du, or equivalently the counterion potential $\delta\mu_+$ for Du $\ll 1$, shows no appreciable ion exchange between the bulk and double layer [Fig. 2(a)]. When Du $\gtrsim 1$, however, bulk counterions follow field lines into or out of the double layer [Fig. 2(b)], as argued physically in Fig. 1(c). The corresponding electric potential $\delta\phi$ for Du = 100 is neither no-flux nor equipotential [Fig. 2(c)]; furthermore, the salt concentration δc shows that counterion flux into or out of the double layer creates local sinks or sources of salt between roughness maxima, driving chemiosmotic slip $\mathbf{u}_{\rm CO}$ [Fig. 2(d)].

Velocity fields, normalized by $u_{\rm HS}^{\infty}$, are shown in Figs. 2(e) and 2(f) for Du = 0.01 and Du = 100, respectively. For Du = 0.01, the local slip velocity $u_\parallel$ is inhomogeneous [as in Fig. 1(b)], but the far-field velocity $\mathbf{U}_{\rm EO}^{\infty}$ is essentially identical to $\mathbf{u}_{\rm HS}^{\infty}$, reflecting similitude [9,10]. At high Du, the slip velocity $u_\parallel \approx u_{\rm HS}^{\infty}/\Lambda$ is essentially constant as counterion transport in the double layer becomes rate-limited by exchange with the bulk [as in Fig. 1(d)].

Figure 3(a) shows the counterion contribution to the far-field electrokinetic velocity $\mathbf{U}_{\rm EO}^{\rm ctr}$, normalized by the counterion contribution to the Helmholtz-Smoluchowski slip velocity $u_{\rm HS}^{\rm ctr}$, at varying Du and roughness amplitudes a_r/L. The coion contribution to the far-field velocity, $\mathbf{U}_{\rm EO}^{\rm co}$, may be computed separately and simply added to $\mathbf{U}_{\rm EO}^{\rm ctr}$. In particular, coions obey an effective no-flux boundary condition (9), so that similitude [9] allows $\mathbf{U}_{\rm EO}^{\rm co}$ to be computed without regard for surface geometry. As shown in Fig. 3(b) (inset), $\mathbf{U}_{\rm EO}^{\rm co} \leq \ln(4)$ for all Du [21], and is thus generally weaker than $\mathbf{U}_{\rm EO}^{\rm ctr}$. For Du $\ll 1$, $\mathbf{U}_{\rm EO}^{\infty} \approx \mathbf{u}_{\rm HS}^{\infty}$, but for Du $\sim \mathcal{O}(1)$, $\mathbf{U}_{\rm EO}^{\infty}$ is suppressed as a_r/L increases. For Du $\gg 1$, the tangential slip velocity $u_\parallel$ asymptotes to a constant value given by (3). Solving for the flow due to a sliding wall boundary condition ($u_\parallel = u_{\rm HS}^{\infty}/\Lambda$) yields quantitative agreement with the full computation for $\mathbf{U}_{\rm EO}^{\rm ctr}$ as Du $\rightarrow \infty$ [diamonds in Fig. 3(a)], consistent with Fig. 1(d).

Since inhomogeneities in surface current are driven by surface curvature, we define an alternate Dukhin number, $\mathrm{Du}_R = \sigma_s/(\sigma_b R)$, where R is the radius of curvature at roughness maxima [Fig. 3(b)]. Plotting $\mathbf{U}_{\rm EO}^{\rm ctr}$ vs Du_R reveals a remarkable collapse of the results [Fig. 3(a)]. For $\mathrm{Du}_R \lesssim 1$, $\mathbf{u}_{\rm HS}^{\infty}$ holds until surface conduction begins to influence ion transport. The first such effects occur at surface geometry maxima [Fig. 2(e)], whose curvature R thus gives the relevant length scale for Du_R. $\mathbf{U}_{\rm EO}^{\rm ctr}$ for different a_r/L thus collapse onto one master curve until $\mathrm{Du}_R \gtrsim \mathcal{O}(1)$, whereupon the geometry of the entire surface becomes relevant. At this point, the surface current

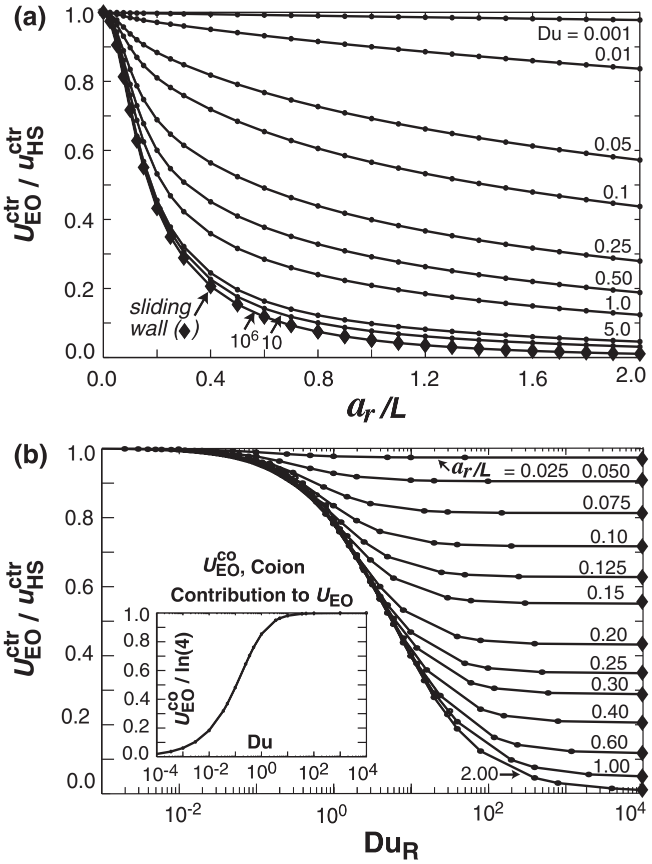

FIG. 3. (a) Counterion contribution to the far-field electro-osmotic slip velocity $\mathbf{U}_{EO}^{ctr}$ vs roughness amplitude a_r/L at varying Du, normalized by $\mathbf{u}_{HS}^{ctr}$. (b) $\mathbf{U}_{EO}^{ctr}/u_{HS}^{ctr}$ plotted against $\mathrm{Du}_R = \sigma_s/(\sigma_b R)$ for various a_r/L. The data collapse onto a master curve for $\mathrm{Du}_R \lesssim 1$ then asymptote to the sliding wall values (◆) as $\mathrm{Du}_R \rightarrow \infty$. Inset: Coion contribution $\mathbf{U}_{EO}^{co}$ vs Du, which is independent of surface geometry.

becomes divergence-free, yielding the sliding wall velocity (diamonds) for each specific geometry as $\mathrm{Du}_R \rightarrow \infty$.

We have shown here that surface roughness can effectively suppress electrokinetic flows and clearly elucidated the central physical mechanism by which it occurs. Although roughness is generally $\mathcal{O}$ (nm) for microfabricated metal electrodes and thus "invisible" on macroscopic length scales, we have shown it can significantly reduce velocities whenever excess surface conductivity is appreciable [$\mathrm{Du}_R \sim \mathcal{O}(1)$], even for thin double layers and constant ζ. The physics behind the mechanism we present here are quite general—essentially requiring only ion conservation—and depend on geometry and excess surface conductivity within the double layer rather than any particular model of the double layer. Although we have here explicitly employed the Gouy-Chapman model of the double layer—as is conventional and classical—our analyses will hold more generally. Including static or dynamic Stern layers [17], ion steric effects [3,5,6], or electroviscous effects [6], for example, will affect the specific dependence of both Du and $\mathbf{u}_{\parallel}$ upon ζ. Nevertheless, we expect far-field electro-osmotic velocities $\mathbf{U}_{EO}^{ctr}$, when scaled by the appropriate u_{HS}^{ctr} and plotted against the relevant Du_R, to collapse as in Fig. 3.

We acknowledge support from the U.S. Department of Energy through the Los Alamos National Laboratory/UCSB Institute for Multiscale Materials Studies, NSF CAREER (CBET-0645097), and the UCSB-ARO Institute for Collaborative Biotechnologies.

---

*squires@engineering.ucsb.edu

[1] T. Squires and S. Quake, Rev. Mod. Phys. **77**, 977 (2005); R. B. Schoch, J. Han, and P. Renaud, Rev. Mod. Phys. **80**, 839 (2008).
[2] W. Russel, D. Saville, and W. R. Schowalter, *Colloidal Dispersions* (Cambridge University Press, Cambridge, England, 1989).
[3] M. Z. Bazant, M. S. Kilic, B. D. Storey, and A. Ajdari, Adv. Colloid Interface Sci. **152**, 48 (2009).
[4] T. M. Squires and M. Z. Bazant, J. Fluid Mech. **509**, 217 (2004); M. Z. Bazant and T. M. Squires, Phys. Rev. Lett. **92**, 066101 (2004).
[5] C. Santangelo, Phys. Rev. E **73**, 041512 (2006).
[6] M. Z. Bazant, M. S. Kilic, B. D. Storey, and A. Ajdari, New J. Phys. **11**, 075016 (2009).
[7] A. J. Pascall and T. M. Squires, Phys. Rev. Lett. **104**, 088301 (2010).
[8] J. Duval, J. Colloid Interface Sci. **269**, 211 (2004).
[9] F. Morrison, J. Colloid Interface Sci. **34**, 210 (1970).
[10] E. B. Cummings, S. J. Griffiths, R. H. Nilson, and P. H. Paul, Anal. Chem. **72**, 2526 (2000).
[11] Y. Hu, C. Werner, and D. Li, Anal. Chem. **75**, 5747 (2003); Y. Hu, C. Werner, and D. Li, J. Colloid Interface Sci. **280**, 527 (2004); Y. Hu, X. Xuan, C. Werner, and D. Li, Microfluid. Nanofluid. **3**, 151 (2007).
[12] M. Wang, J. Wang, and S. Chen, J. Comput. Phys. **226**, 836 (2007); S. Kang and Y. K. Suh, Microfluid. Nanofluid. **6**, 461 (2009).
[13] M. Wang and Q. Kang, Anal. Chem. **81**, 2953 (2009).
[14] D. Kim and E. Darve, Phys. Rev. E **73**, 051203 (2006); R. Qiao, Microfluid. Nanofluid. **3**, 33 (2006).
[15] J. Bikerman, Trans. Faraday Soc. **35**, 154 (1940).
[16] S. S. Dukhin and B. V. Deryaguin, *Surface and Colloid Science* (Wiley, New York, 1979), Vol. 7.
[17] J. Lyklema, *Fundamentals of Interface and Colloid Science* (Academic, London, 1995), Vol. 2.
[18] R. O'Brien, J. Colloid Interface Sci. **92**, 204 (1983); R. O'Brien and L. White, J. Chem. Soc., Faraday Trans. 2 **74**, 1607 (1978).
[19] C. Nogues and M. Wanunu, Surf. Sci. **573**, L383 (2004); A. Mahapatro, A. Scott, A. Manning, and D. Janes, Appl. Phys. Lett. **88**, 151917 (2006).
[20] See supplementary material at http://link.aps.org/supplemental/10.1103/PhysRevLett.105.144503 for derivation of the governing equations.
[21] A. S. Khair and T. M. Squires, Phys. Fluids **21**, 042001 (2009).